PHYSICAL REVIEW B VOLUME 55, NUMBER 11 15 MARCH 1997-I

Isoelectronic bound-exciton photoluminescence in strained beryllium-doped $Si_{0.92}Ge_{0.08}$ epilayers and $Si_{0.92}Ge_{0.08}$/Si superlattices at ambient and elevated hydrostatic pressure

Sangsig Kim, Ganlin Chang, and Irving P. Herman
Department of Applied Physics and Columbia Radiation Laboratory, Columbia University, New York, New York 10027

Joze Bevk
Lucent Technologies, Bell Laboratories, Murray Hill, New Jersey 07974

Karen L. Moore and Dennis G. Hall
The Institute of Optics, University of Rochester, Rochester, New York 14627

(Received 19 August 1996)

Photoluminescence (PL) from a beryllium-doped $Si_{0.92}Ge_{0.08}$ epilayer and three different beryllium-doped $Si_{0.92}Ge_{0.08}$/Si superlattices (SL's) commensurately grown on Si(100) substrates is examined at 9 K at ambient pressure and, for the epilayer and one SL, as a function of hydrostatic pressure. In each structure, excitons bind to the isoelectronic Be pairs in the strained $Si_{0.92}Ge_{0.08}$ layers. The zero-phonon PL peaks of the epilayer and the *in situ* doped 50-Å $Si_{0.92}Ge_{0.08}$/100-Å Si SL shift linearly with pressure toward lower energy at the rate of 0.68 ± 0.03 and 0.97 ± 0.03 meV/kbar, respectively, which are near the 0.77-meV/kbar value for Si:Be. The PL energies at ambient and elevated pressure are analyzed by accounting for strain, quantum confinement, and exciton binding. A modified Hopfield-Thomas-Lynch model is used to model exciton binding to the Be pairs. This model, in which potential wells bind electrons to a site (that then trap holes), predicts a distribution of electron binding energies when an inhomogeneous distribution of potential-well depths is used. This accounts for the large PL linewidth and the decrease of linewidth with increasing pressure, among other observations. In SL's, the exciton binding energy is shown to depend on the width of the wells as well as the spatial distribution of Be dopants in the superlattice. Also, at and above 58 kbar a very unusual peak is observed in one of the SL's, which is associated with a free-exciton peak in Si, that shifts very fast with pressure (-6.02 ± 0.03 meV/kbar). [S0163-1829(96)09648-8]

I. INTRODUCTION

The introduction of isoelectronic impurities into indirect-band-gap semiconductors helps improve the quantum efficiency of optical emission. In particular, zero-phonon emission from bulk Si, a $Si_{0.92}Ge_{0.08}$ alloy, and $Si_{0.92}Ge_{0.08}$/Si superlattices (SL's) becomes very strong when isoelectronically doped by Be pair acceptors, compared to that from their undoped analogs.[1–3] Such strong emission suggests the possibility of IR light-emitting diodes fabricated using these beryllium-doped semiconductors.[4]

In bulk Si:Be, non-Coulomb interactions (or more precisely nonionic interactions) dominate in binding excitons to the dipolar, isoelectronic substitutional-interstitial (SI) pairs of Be atoms.[5] Reference 5 described this binding mechanism by modifying the Hopfield-Thomas-Lynch (HTL) approach[6] for excitons bound to single atomic isoelectronic dopants. An electron is trapped in the non-Coulomb short-range potential created by the Be SI pair, and the hole binds to the trapped electron through Coulomb interactions to form a bound exciton.

The photoluminescence (PL) spectrum of Be-doped $Si_{1-x}Ge_x$ alloys[1–3,7] differs from that in the more-widely studied undoped alloys.[8–11] The near-band-gap zero-phonon PL emission from undoped $Si_{1-x}Ge_x$ alloys has the following characteristics:[9] (1) the PL energy tracks the band gap, (2) line-shape broadening is due to variations in the band-gap energy caused by local fluctuations in the alloy composition, and (3) the intensity of the zero-phonon emission relative to that of phonon replicas increases with the mole fraction x, from 0 for $x=0$ (Si) to a maximum of $x=0.5$. In contrast, for the zero-phonon emission from strained $Si_{1-x}Ge_x$:Be alloys, (1) the PL energy shifts with composition at a rate slower than that of the band gap,[1] (2) the linewidth is much broader than that for undoped, unstrained alloys; and (3) the ratio of the intensity of the zero-phonon peak to that of the phonon replicas decreases with increasing mole fraction x. These differences are due to the fundamental differences in exciton binding in these undoped and isoelectronically doped semiconductors.

Zero-phonon PL emission occurs in the undoped alloys when electrons at X valleys ($0<x<0.85$) are scattered because of the random arrangement of Si and Ge atoms.[8,9] Some of the scattered electrons have Γ components in wave-vector space and can combine with holes in the Γ valley without emitting phonons. In contrast, for the Be-doped alloys, most of the localized electrons trapped in the short-range potential exist at X-band valleys, but their wave functions have tails near the Γ point in k space because of their tight spatial localization.[12,13] Zero-phonon emission comes from the recombination due to the overlap of the tails of the wave function of the electrons and the holes in the Γ valley. In Ref. 5, hydrostatic pressure was shown to alter the strength of the trapping of electrons to the Be pairs in Si.

0163-1829/97/55(11)/7130(11)/$10.00

TABLE I. Energy positions of the zero-phonon peak (meV).

Name	Description[a]	Doped region	E_{PL} (measured)	E_{PL} (predicted)	E_{cf} (calculated)	E_{e-h} (calculated)[b]	E_e
Epilayer	4800-Å SiGe	SiGe	1034		0	38	25
SL-*A*	10×(50-Å SiGe/100-Å Si)	Middle 17 Å of SiGe	1040	1040	18	50	25
SL-*B*	20×(20-Å SiGe/100-Å Si)	Middle 11 Å of SiGe	1062[c]	1060	45	57	25
SL-*C*	40×(50-Å SiGe/100-Å Si)	SiGe and Si	1051	1046	18	44	25

[a] All SiGe alloys have composition $Si_{0.92}Ge_{0.08}$, and are grown commensurately on Si(100).

[b] Asumming $m_h = 0.38 m_0$.

[c] The lower-energy zero-phonon peak.

This binding mechanism might be different in $Si_{1-x}Ge_x$, both at ambient and elevated pressures.

The coherent strain in the $Si_{1-x}Ge_x$ epilayer generated by lattice mismatch between the epilayer and the Si(100) substrate reduces the indirect band gap of the alloy, and splits the conduction and valence bands.[14,15] For strained, undoped $Si_{1-x}Ge_x$ epilayers, both the reduction of the band gap and the splitting of the valence band caused by biaxial strain change the PL energy.[11,16] Similarly, the biaxial strain is expected to affect the PL peak position and width of strained $Si_{1-x}Ge_x$:Be epilayers at ambient pressure.[17] Furthermore, the biaxial strain is modified with the application of hydrostatic pressure because the alloy and Si substrate have different bulk moduli.[17]

In this paper, PL from a $Si_{0.92}Ge_{0.08}$ epilayer and $Si_{0.92}Ge_{0.08}$/Si superlattices, each doped isoelectronically by Be, is examined and compared to that in bulk, unstrained Si:Be, both at ambient and elevated hydrostatic pressure. In each of these heterostructures the exciton emission comes from the $Si_{0.92}Ge_{0.08}$ epilayers, each of which is compressively strained (the same way) during commensurate growth on Si(100). The mechanism of exciton binding is analyzed using the PL measurements, taking into account changes in band structure due to alloying, strain, and quantum confinement, and the different spatial distributions of the Be isoelectronic dopant. The experimental procedure and results are presented in Sec. II. Section III separately discusses the observations at ambient (Sec. III A) and elevated hydrostatic pressure (Sec. III B), and details a model of exciton binding in SiGe:Be alloys (Sec. III C). Concluding remarks are presented in Sec. IV. Preliminary analysis of PL from these structures at ambient pressure can be found in Refs. 1–3.

II. EXPERIMENTAL PROCEDURE AND RESULTS

Be ions (40 keV) were implanted into a 4500-Å-thick strained $Si_{0.92}Ge_{0.08}$ epilayer, grown by molecular-beam epitaxy (MBE) onto a Si(100) substrate, with a dose of 2×10^{13} ions/cm^2.[3] This sample was annealed at 590 °C for 10 min. Three strained SL's were grown by MBE on Si(100). SL-*A*, with ten periods of 50-Å $Si_{0.92}Ge_{0.08}$/100-Å Si, and SL-*B*, with 20 periods of 20-Å $Si_{0.92}Ge_{0.08}$/100-Å Si, were doped *in situ* with Be during MBE in the middle 17 and 11 Å of their SiGe wells, respectively.[3] SL-*C*, with 40 periods of 50-Å $Si_{0.92}Ge_{0.08}$/100-Å Si, was implanted with 2×10^{13} ions/cm^2 after growth to introduce Be throughout the SiGe and Si layers, and was then annealed (Table I).[2]

Photoluminescence was measured at 9 K in a diamond-anvil cell loaded with liquid argon.[5,17] Two ruby chips were placed inside the hole of the gasket along with the thinned sample to assess pressure uniformity and to calibrate pressure. PL was excited by the 514-nm line from an argon-ion laser (15 mW), which was chopped at 104 Hz. The PL was dispersed by a 0.85-m double spectrometer, detected by a Ge detector, and analyzed by lock-in analysis. PL was examined from the four samples at ambient pressure and from only the epilayer and SL-*A* at elevated pressures. The PL spectra of these latter two structures were the same (at 1 bar) before applying pressure and after the release of pressure.

PL spectra of the $Si_{0.92}Ge_{0.08}$:Be epilayer are shown in Fig. 1 at selected pressures. Each spectrum has a large asymmetric peak at high energy that is resolved, using Pearson-VII functions,[5,18] into a strong zero-phonon peak at higher energy and a weaker peak attributed to the TA/*P* phonon replica at lower energy; the *P* phonon replica corresponds to an unidentified phonon replica reported for Si:Be in Ref. 5. (Pearson-VII peak-fitting functions can vary between the Gaussian and Lorentzian line shapes.) Each epilayer spectrum also has a second peak at lower energy attributed to the TO-phonon replica. All of the phonon replicas seen here in $Si_{0.92}Ge_{0.08}$:Be correspond to Si-Si modes.

At ambient pressure, the PL line shapes of the three SL's are similar to that of the epilayer (Fig. 2), except that two distinct peaks are seen in the zero-phonon region of the narrow well, *in situ*-doped SL-*B*. The lower energy peak in SL-*B* appears to be due to the heavy-hole (hh) exciton. Although the separation of these two peaks (11 meV) in SL-*B* is on the order of the calculated hh/lh (light-hole) splitting (18 meV,

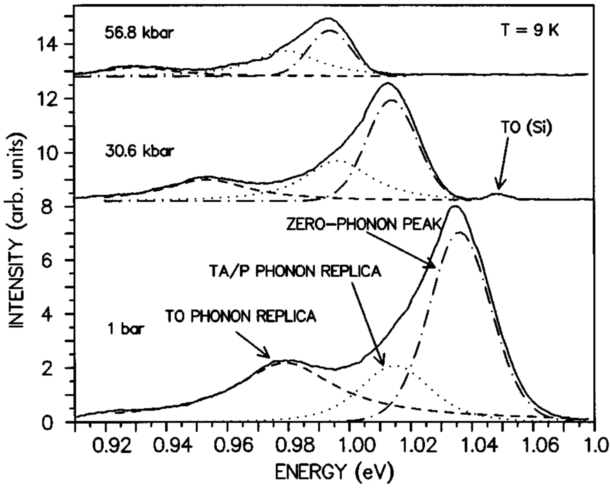

FIG. 1. PL spectra of the $Si_{0.92}Ge_{0.08}$:Be epilayer at selected pressures, fitted using Pearson-VII functions (9 K).

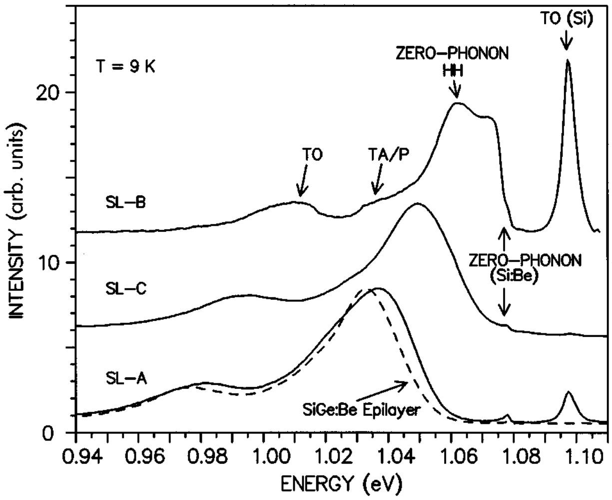

FIG. 2. PL spectra of the $Si_{0.92}Ge_{0.08}$:Be epilayer and the three beryllium-doped SL's at ambient pressure (9 K).

including strain and confinement terms), k_BT (1 meV) is too small for significant thermal population of the light-hole state. This conclusion is substantiated by measurements showing that the relative intensity of the two peaks does not change from 9 to 30 K.

The PL spectra of the epilayer and SL-*A* and SL-*C* were fitted using three Pearson-VII functions. The zero-phonon peak for both superlattices is due to the recombination of the hh exciton, and the phonon replica identifications are the same as for the epilayer. The PL spectrum of SL-*B* was fitted to four peaks. The peak energies for the SL's are listed in Table I. The PL energies of the three SL's are distinct, and each is higher than the corresponding peaks in the epilayer; these differences are explained in terms of confinement and exciton binding energies in Sec. III A 2. The full width at half maximum (FWHM) of the zero-phonon peaks has an uncertainty of ~2 meV because of overlap with the TA/*P* peaks. A small, narrow peak at 1.078 eV is seen in the four samples, which is at the same energy as zero-phonon PL in Si:Be and is attributed to excitons bound to Be pairs in Si layers (even in the *in situ*-doped SL's) and/or the Si substrate.

Figure 3 plots the peak energies of the epilayer PL spectral features as a function of hydrostatic pressure. The pressure dependence of the peak energy (E) of each feature is characterized by fitting the data to

$$E(P)=E_0(P=1\,\text{bar})+\alpha P, \qquad (1)$$

where P is the pressure in kbar. The fitting constants are listed in Table II. The parameter $\alpha(=dE/dP)$ for the zero-phonon peak of this strained $Si_{0.92}Ge_{0.08}$:Be epilayer (−0.68 meV/kbar) is smaller in magnitude than that for bulk Si:Be (−0.77 meV/kbar).[5] The splitting between the zero-phonon peak and the TO-phonon replica increases with pressure, while that between it and the TA/P-phonon replica decreases with pressure. The normalized and energy-shifted spectra in Fig. 4 (for P up to 56.8 kbar) show this, and also that the FWHM of the main asymmetric peak decreases with increasing pressure. The epilayer PL intensity decreases with pressure; there is no PL at and above 64.2 kbar (Fig. 5). (In Si:Be the integrated PL intensity remained roughly constant up to ~50 kbar and then decreased rapidly.[5])

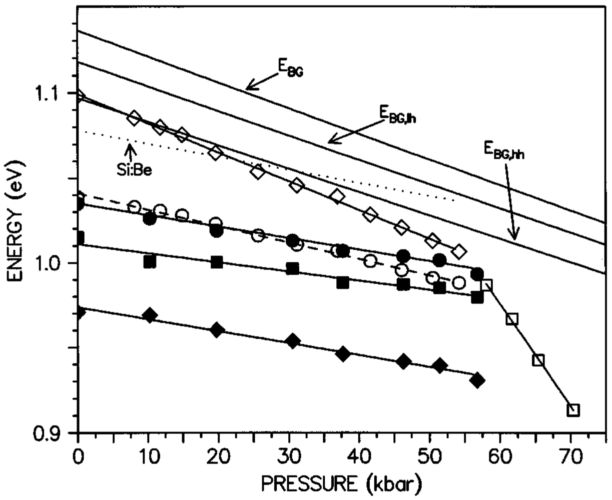

FIG. 3. The dependence of the PL energies of the $Si_{0.92}Ge_{0.08}$:Be epilayer [the zero-phonon peak (●), TA/P-phonon replica (■), and TO phonon replica (◆)] and SL-*A* [the zero-phonon peak (○), TO-phonon replica associated with free excitons in Si (◇), and the PX peak (□)], as a function of pressure at 9 K. See Table II for the curve fitting parameters. The pressure dependencies of the indirect band gap (E_{BG}, for an unstrained alloy), the hh and lh band gaps ($E_{BG,hh}$ and $E_{BG,lh}$ for the strained alloy), and the zero-phonon peak of Si:Be (dotted line) are shown for comparison.

PL spectra from SL-*A* at selected pressures are displayed in Fig. 6. The pressure dependence of the zero-phonon peak energy is characterized using Eq. (1) to give the fitting constants listed in Table II. The peak energy is plotted as a function of hydrostatic pressure in Fig. 3, along with the fit. The magnitude of α for the SL-*A* zero-phonon peak is larger than that for Be-doped bulk Si and the $Si_{0.92}Ge_{0.08}$:Be epilayer. The integrated intensity of the zero-phonon SL-*A* peak

TABLE II. Energy positions and pressure coefficients for the PL peaks, using the fit of Eq. (1).

	$E(0)$ (eV)	α (meV/kbar)
Epilayer		
SiGe zero phonon	1.035±0.001	−0.68±0.3
SiGe TA/P-phonon replica	1.011±0.002	−0.54±0.6
SiGe TO-phonon replica	0.974±0.002	−0.71±0.4
SL-*A*		
SiGe zero phonon	1.041±0.001	−0.97±0.03
SiGe TO-phonon replicas of free excitons	1.099±0.002	−1.70±0.03
Si PX (P<58 kbar)	1.337±0.002	−6.02±0.03
Si:Be peak A[a]	1.078	−0.77
Strained SiGe hh gap	1.097	−1.38
Strained SiGe lh gap	1.118	−1.43
Unstrained SiGe indirect gap	1.136	−1.50

[a] From Ref. 5.

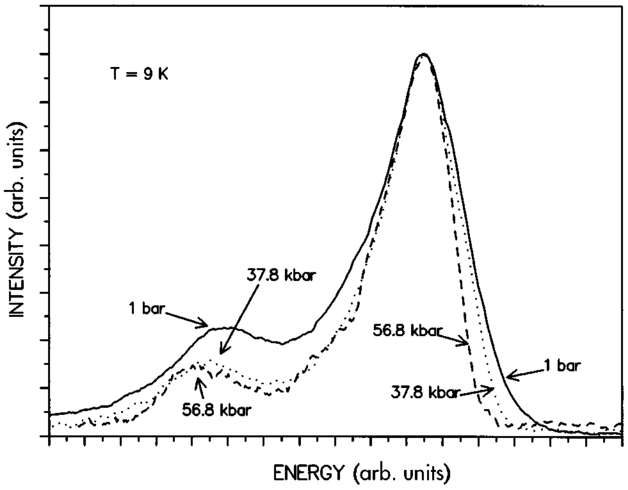

FIG. 4. PL spectra of the $Si_{0.92}Ge_{0.08}$:Be epilayer at selected pressures, with the zero-phonon peaks of each shifted to the same energy and normalized to the same height (9 K).

decreases with increasing pressure with the same dependence as that in the epilayer; no zero-phonon peak is seen at and above 58.1 kbar.

At ambient pressure, the TO-phonon replica of the free-exciton (FE) recombination in Si is very strong in the *in situ*-doped SL-*A* and SL-*B*, and is attributed to recombination in either the Si barriers or substrate, while it is very weak in the samples doped by implantation: the epilayer and SL-*C* (Fig. 2), and bulk Si:Be (Ref. 5). TO-phonon replicas of free excitons from the $Si_{0.92}Ge_{0.08}$ wells and zero-phonon free excitons in Si and SiGe are not seen in any sample. The pressure dependence of the TO-phonon replica of (Si) free excitons in SL-*A* is the same as that of the band gap in Si for pressures up to 54 kbar. However, at higher pressures the peak correlating with this phonon replica has a very different pressure (and large) coefficient (−6.02 meV/kbar) (Fig. 3); at these pressures it may correspond to a different feature, which will be called *PX*. This (Si) TO-phonon replica is seen at lower pressures in the other samples. However, it merges into the strong zero-phonon peak at higher pressures, and in contrast to the measurements in SL-*A*, the ''new'' peak is not observed—even at higher pressures when the zero-phonon peak from SiGe:Be disappears.

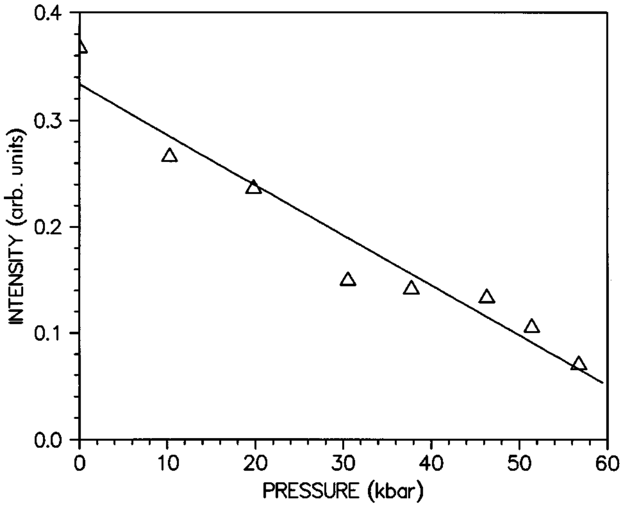

FIG. 5. The pressure dependence of the integrated PL intensity in the epilayer at 9 K.

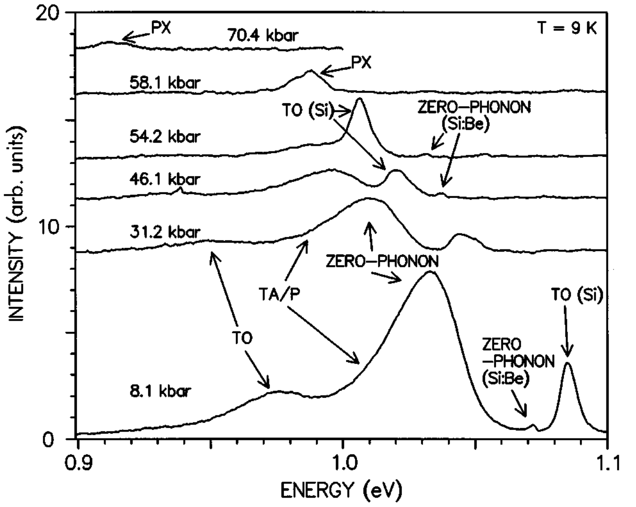

FIG. 6. PL spectra of SL-*A* [*in situ* doped, 10×(50-Å $Si_{0.92}Ge_{0.08}$/100-Å Si)] at selected pressures (9 K).

III. DISCUSSION

A. PL at ambient pressure

1. PL energies in the strained $Si_{0.92}Ge_{0.08}$:Be epilayer

The band gap of a biaxially compressed strained $Si_{0.92}Ge_{0.08}$ epilayer grown on Si(100) is smaller than of the unstrained alloy due to its contracted volume and the shear stress-induced splitting of the conduction and valence bands.[14,15] The biaxial strain in the plane of the layer is

$$\varepsilon_{xx}^{(b)}=\varepsilon_{yy}^{(b)}=\frac{a_{\mathrm{Si}}}{a}-1, \tag{2}$$

and that normal to the layer is

$$\varepsilon_{zz}^{(b)}=-\frac{2C_{12}}{C_{11}}\,\varepsilon_{xx}^{(b)}, \tag{3}$$

where a and a_{Si} are the lattice constants for the relaxed alloy and Si, and C_{ij} are the alloy elastic constants. The change of the band gap due to the concomitant hydrostatic strain $\Delta E_{\mathrm{BG}}^{\varepsilon}$ is

$$\Delta E_{\mathrm{BG}}^{\varepsilon}(P)=2a_h\left(1-\frac{C_{12}}{C_{11}}\right)\varepsilon^{(b)}(P), \tag{4}$$

where a_h is the hydrostatic deformation potential of the alloy (1.50 eV).[15]

The biaxial strain shifts the heavy- and light-hole bands at the Γ point by ΔE_{hh} and ΔE_{lh} relative to the center of gravity of the valence band, where

$$\Delta E_{\mathrm{hh}}=-\tfrac{1}{2}\,\delta E_{001} \tag{5}$$

and

TABLE III. Parameters of Si, Ge, and $Si_{0.92}Ge_{0.08}$.

	Si	Ge	$Si_{0.92}Ge_{0.08}$
B (kbar)	980	728	960
a_0 (Å)	5.431	5.657	5.449
m_h (m_0)	0.4	0.2	0.38
ε_0	11.4	15.36	11.7
b (eV)	-2.35	-2.55	-2.37
Ξ_u^Δ (eV)	9.16	9.42	9.18
a_h (eV)	1.50	1.50	1.50
C_{12}/C_{11}	0.388	0.376	0.387
Δ_0 (eV)	0.044	0.29	0.064

$$\Delta E_{\mathrm{lh}} = -\tfrac{1}{2}\Delta_0 + \tfrac{1}{4}\delta E_{001} + \tfrac{1}{2}(\Delta_0^2 + \Delta_0 \delta E_{001} + \tfrac{9}{4}(\delta E_{001})^2)^{1/2}. \tag{6}$$

Δ_0 is the spin-orbit splitting, and is assumed to be equal to 64 meV, independent of pressure.[17] δE_{001} is the splitting due to strain (Table III),

$$\delta E_{001} = -2b\left(1 + \frac{2C_{12}}{C_{11}}\right)\varepsilon_{xx}^{(b)}, \tag{7}$$

where b is the shear deformation potential (-2.37 eV).[15]

Similarly, biaxial strain shifts the conduction bands along [100] and [010] by $\Delta E_c^{100,010}$, and that along [001] by ΔE_c^{001}, relative to the center of gravity, where

$$\Delta E_c^{100,010} = \frac{1}{3}\Xi_u^\Delta\left(1 + \frac{2C_{12}}{C_{11}}\right)\varepsilon^{(b)} \tag{8}$$

and

$$\Delta E_c^{001} = -\tfrac{2}{3}\Xi_u^\Delta\left(1 + \frac{2C_{12}}{C_{11}}\right)\varepsilon^{(b)}. \tag{9}$$

Ξ_u^Δ is the deformation potential for the conduction-band valley at point Δ (9.18 eV).[15]

For biaxially compressive strain, the [100] and [010] bands are the lowest conduction bands, and the heavy hole is the highest valence band. The hh (lh) band gap of the strained alloy, $E_{\mathrm{BG,hh(lh)}}$, is defined by the difference between $E_c^{100,010}$ and $E_{\mathrm{hh(lh)}}$,[14,15,17]

$$E_{\mathrm{BG,hh(lh)}} = E_{\mathrm{BG}} + \Delta E_{\mathrm{BG}}^{\varepsilon} - \Delta E_c^{100,010} - \Delta E_{\mathrm{hh(lh)}}, \tag{10}$$

where E_{BG} is the indirect band gap of the unstrained $Si_{0.92}Ge_{0.08}$ alloy.

The indirect band gap of the unstrained $Si_{0.92}Ge_{0.08}$ alloy is found to be 1.135 eV from the energy of free-exciton PL in unstrained $Si_{1-x}Ge_x$ ($0 \leq x \leq 0.85$) (Ref. 8) and the binding energy of the free exciton, which is estimated by a linear interpolation between the binding energies of the FE in Si and Ge (Table III). $E_{\mathrm{BG,hh}}$ and $E_{\mathrm{BG,lh}}$ are estimated to be 1.097 and 1.118 eV using Eq. (10).

The binding energy (E_{ex}) of an exciton bound to an isoelectronic acceptor is the binding energy of the trapped electron (E_e), plus the energy required to remove the hole from this trapped electron ($E_{e\text{-}h}$).[5] If the zero-phonon PL peak is due to the hh exciton, the PL energy (E_{PL}) is

$$E_{\mathrm{PL}} = E_{\mathrm{BG,hh}} - E_e - E_{e\text{-}h}. \tag{11}$$

Using the model presented in Ref. 5, $E_{e\text{-}h}$ is 42 meV in Si:Be (at and above ambient pressure) when the electron is treated as point, which agrees with the experimental value (43 meV). Using the dielectric constant and hole mass $m_h = 0.38m_0$ for the $Si_{0.92}Ge_{0.08}$:Be alloy, $E_{e\text{-}h} = 38$ meV, where an average hole mass is assumed and m_0 is the mass of a free electron. Equation (11) then gives $E_e = 25$ meV for the epilayer, which is much smaller than the value of 48 meV determined for Si:Be. (Using $m_h = 0.50m_0$, which is an estimate of the angle-averaged mass of the heavy hole in this alloy, $E_{e\text{-}h} = 52$ meV and $E_e = 14$ meV.)

This smaller electron binding energy in the alloy is consistent with a spatial variation of binding energy due to the varying local composition in the alloy. In Si, the isoelectronic pairs of Be atoms occupy substitutional and interstitial sites (along [111]).[5] In SiGe, the Be pairs experience varying local chemical compositions (of Si or Ge atoms) and strains, leading to a range of E_e. (It is also possible that orientations of the pair other than [111] may occur in the alloy.) The large PL linewidth in $Si_{0.92}Ge_{0.08}$:Be (Sec. II) and the increase in linewidth with x (Ref. 1) are consistent with this microscopic variation in E_e. This decrease of the average observed E_e with alloying by Ge suggests that the presence of Ge atoms decreases the binding energy either because of changes in the binding potential or the concomitant disorder. This conclusion is also consistent with the decreased PL linewidth and intensity with increasing pressure (Sec. II).

More generally, the variation of the average exciton binding energy with Ge content can be obtained from the difference in the known variation in the band gap in strained $Si_{1-x}Ge_x$ layers grown on Si(100) (Ref. 9) and the measured PL energy in strained $Si_{1-x}Ge_x$:Be epilayers.[1] This gives $d(E_e + E_{e\text{-}h})/dx = -262$ meV for small x. Using the variation in ε and m_h with x, the model for electron-hole binding in Ref. 5 (for pointlike electrons) gives $dE_{e\text{-}h}/dx = -50$ meV for $m_h = 0.38m_0$ (and -33 meV for $m_h = 0.50m_0$). Therefore, $dE_e/dx = -212$ meV (-229 meV). If there were only one type of binding site, this would predict that no binding should occur for $x > 0.23$. Actually, there will be some binding in these Ge-rich alloys because of the inhomogeneous distribution of different binding sites. Section III C presents a model that is able to describe many of the reported observations, by assuming such a distribution.

2. Comparison of PL energies in the epilayer and superlattices

Comparison of zero-phonon PL of the SL's and the epilayer is appropriate, since superlattice PL comes from SiGe wells and the SiGe layers in each heterostructure have the same strain.[2,3] At ambient pressure, the PL energy of SL-*A* exceeds that for the epilayer by 6 meV, which is less than the confinement energy expected for the SL structure. Although SL-*A* and SL-*C* have the same structure, their PL spectra are different, which suggests that the total binding energies of the bound excitons depend on the spatial distribution of Be dopants. Clearly, the binding energy of the bound exciton and the confinement energy are both important factors in determining the PL energy. The PL energy (E_{PL}) of the zero-phonon peak in a SL is

$$E_{\mathrm{PL}} = E_{\mathrm{BG,hh}} + E_{\mathrm{cf}} - E_e - E_{e\text{-}h}, \tag{12}$$

where E_{cf} is the confinement energy. Since the binding energy E_e of an electron to the Be pair should be independent of both the well width and Be distribution within the $\mathrm{Si_{0.92}Ge_{0.08}}$ wells (because of the negligible conduction-band offset, as explained below), E_e should be the same for each of the four samples. Similarly, $E_{\mathrm{BG,hh}}$ should be the same for all of the structures because the strain is the same for all of the SiGe layers in these samples. Thus the PL energies of the SL's are different, as well as being shifted relative to that in the epilayer, because they have different E_{cf} and $E_{e\text{-}h}$. This is true at both ambient and elevated pressures.

Strained $\mathrm{Si}_{1-x}\mathrm{Ge}_x$/Si SL's grown on Si(100) are reported to have type-I band alignment, and for a $\mathrm{Si_{0.8}Ge_{0.2}}$/Si SL the conduction-band offset is known to be very small ($\Delta E_c = 20$ meV).[19] In recent work, PL from a $\mathrm{Si_{0.83}Ge_{0.17}}$/Si heterojunction was thought to be consistent with either type-I or type-II band alignment, with $\Delta E_c \leqslant 10$ meV.[11] Thus the conduction-band offset in the SL's studied here is assumed to be negligible, and the difference between the band gaps of bulk Si and the strained $\mathrm{Si_{0.92}Ge_{0.08}}$ alloy is the valence-band offset. Then at ambient pressure the hh and lh band offsets are 73 and 52 meV, respectively, and the splitting of the valence band is 21 meV.

SL-*A* and SL-*B* must have type-I alignment, since electrons are tightly bound to the Be complexes that are *in situ* placed in the middle of the wells, and holes are confined in the wells due to the large valence-band offset. In contrast, in SL-*C* electrons are bound to Be complexes that are distributed throughout the SL structure with the same probability in the Si and $\mathrm{Si_{0.92}Ge_{0.08}}$ layers (per monolayer), while most holes are confined within the $\mathrm{Si_{0.92}Ge_{0.08}}$ wells.

The model for a hydrogenic impurity in a finite quantum well proposed by Tanaka, Nagaoka, and Yamabe[20] is used to estimate the confinement and binding energies, assuming that the effective hole mass m_h is spherically symmetric. With a parabolic approximation, the Hamiltonian for holes is[20,21]

$$H = -\frac{\hbar^2}{2m_h}\left[\frac{1}{\rho}\frac{\partial}{\partial\rho}\left[\rho\frac{\partial}{\partial\rho}\right] + \frac{1}{\rho^2}\frac{\partial^2}{\partial\phi^2}\right] - \frac{\hbar^2}{2m_h}\frac{\partial^2}{\partial z^2} - \frac{e^2}{\varepsilon\sqrt{\rho^2+(z-z_i)^2}} + V(z), \tag{13}$$

using cylindrical polar coordinates (ρ,ϕ,z), where $V(z)$ is the periodic potential, ε the dielectric constant, and z_i the coordinate of the impurity site along the superlattice axis. (The charge distribution of the trapped electron is assumed to be pointlike at z_i.) For simplicity, the values of m_h and ε for $\mathrm{Si_{0.92}Ge_{0.08}}$ (Table III) are used both for the wells and barriers.[20] It is assumed that a variational wave function of a hole can be written as the product of a one-dimensional wave function (f) associated with the superlattice potential and a three-dimensional wave function (ψ) due to the local potential[20,21]

$$\Psi(\rho,z,z_i) = f(z)\,\psi(\rho,z-z_i), \tag{14a}$$

$$\psi(\rho,z-z_i) = \exp\left(-\gamma\sqrt{\rho^2+(z-z_i)^2}\right), \tag{14b}$$

where γ is the variational parameter.

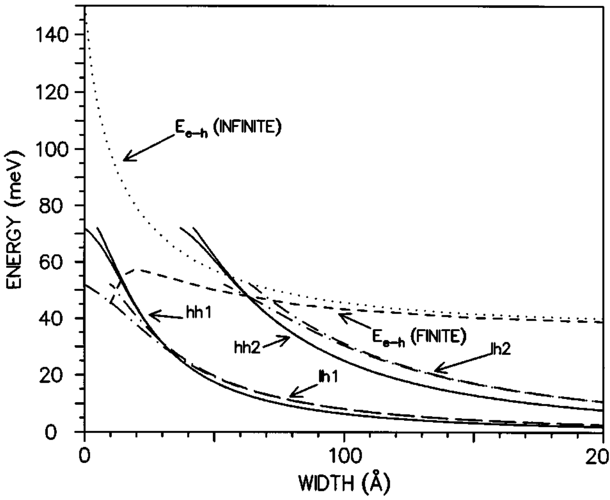

FIG. 7. The binding energies of $E_{e\text{-}h}$ calculated using the infinite (dotted line) and finite (dashed line) models, and the calculated hh and lh confinement energies, as a function of the well width.

Solution of the Schrödinger equation with H from Eq. (13) and Ψ from Eq. (14) by variational analysis gives an eigenvalue equal to $E_{\mathrm{cf}} + E_{e\text{-}h}(z_i)$. If the Coulomb potential term is neglected in Eq. (13), the resulting one-dimensional Schrödinger equation for $f(z)$ can be solved by the Kronig-Penney model[21,22] to give the energy eigenvalue E_{cf}, the confinement energy. The binding energy $E_{e\text{-}h}(z_i)$ is the difference in these eigenvalues.

The confinement energies for the hh and lh are plotted as a function of the well width in Fig. 7. Estimates assuming hole confinement in a single square-potential well[20] give the same result within ±1 meV.

The electron-hole binding energy $[E_{e\text{-}h}(z_i)]$ for heavy holes is plotted in Fig. 7 as a function of the well width, assuming that the Be pair is in the center of the well, along with the result for the infinite-potential-well model.[23] (The variational parameter γ is 1/18 Å.) The infinite-potential-well model[24] is inappropriate for SL's with wells narrower than 100 Å, since the estimated binding energy incorrectly increases exponentially as the width is reduced, because leakage of the hole wave function into the barrier is neglected. The binding energy $E_{e\text{-}h}(z_i)$ is plotted as a function of the distance of the Be pair from the center of the well in Fig. 8, for 50- and 20-Å well widths.

In SL-*A* and SL-*B*, the Be atoms are distributed in the middle 17 and 11 Å of their wells, respectively, and, in SL-*C*, the Be atoms are distributed throughout the alloy and Si layers. The weighted-average binding energy reflects this spatial distribution of Be pairs $g(z_i)$, the binding energy for that site $E_{e\text{-}h}(z_i)$ (Fig. 8), and the probability that there is a hole at that site to be trapped $|f(z_i)|^2$:

$$E_{e\text{-}h} = \frac{\int E_{e\text{-}h}(z_i)\,g(z_i)\,|f(z_i)|^2\,dz_i}{\int g(z_i)\,|f(z_i)|^2\,dz_i}, \tag{15}$$

where the integration is over the width of the well. The weighted-average binding energies of SL-*A*, SL-*B*, and SL-*C* are estimated to be 50, 57, and 44 meV, respectively (Table I).

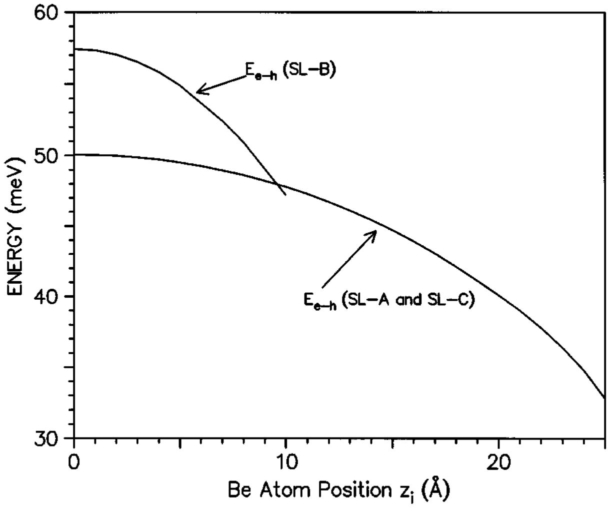

FIG. 8. The binding energies of $E_{e\text{-}h}$ calculated using the finite model, as a function of the Be position in the SL well, for the given well width.

Using Eq. (12), the PL energy positions for SL-*A*, SL-*B*, and SL-*C* are expected to be 1.040, 1.060, and 1.051 eV, respectively (Table I); the measured energies are 1.040, 1.064, and 1.047 eV, respectively.

The zero-phonon region for the narrow-well superlattice (SL-*B*) has two peaks. The lower-energy peak is attributed to the hh exciton. The higher-energy peak is unidentified. Biaxial strain raises the lh band by 21 meV relative to the hh band, while the confinement energy of the lh is 3 meV smaller than that for the hh [in the parabolic approximation, assuming $m_{\text{lh}}=m_{\text{hh}}/3$ (Ref. 25)]. While this would lead to a lh peak at 1.080 eV, close to that of the higher peak (1.073 eV)—assuming that $E_e+E_{e\text{-}h}$ is equal for hh and lh excitons, the lh state will not be populated since the 18-meV separation of the lh and hh bands is $\gg k_BT$ ($\sim$1 meV at 9 K). An alternative origin of this peak attributes it to the $n=2$-hh miniband. However, Fig. 7 shows that only $n=1$ hh is expected for the 20-Å-wide well. Even if the $n=2$-hh miniband existed, any peak associated with this miniband probably would not be strong because of the $\Delta n=0$ selection rule for exciton formation; the conduction-band offset is so shallow that only the $n=1$ electron miniband can exist. The unchanged ratio of the intensities of the peaks at 1.080 and 1.073 eV with changing temperature suggests that the high-energy peak cannot be due to higher-energy electron or hole bands.

3. PL linewidth

The linewidths of the zero-phonon peaks in the strained $\text{Si}_{1-x}\text{Ge}_x$:Be epilayers are much wider than those in the undoped, unstrained alloy.[1,9] In particular, the linewidth (FWHM) for the strained $\text{Si}_{0.92}\text{Ge}_{0.08}$:Be epilayer is 22 meV (for SL-*A* it is 21 meV), while for undoped (strained or unstrained) $\text{Si}_{0.92}\text{Ge}_{0.08}$ layers it is 7 meV. (The PL linewidth in Si:Be is $\sim$1 meV.) Most of the linewidth of the peak in unstrained, undoped $\text{Si}_{1-x}\text{Ge}_x$ is due to the variation of the band-gap energy with local composition.[8,26] In the strained, doped alloy, the peak is broadened further by spatial inhomogeneity in the binding energies E_e and $E_{e\text{-}h}$.[27]

The variations in the binding energies of the trapped electron and hole, ΔE_e and $\Delta E_{e\text{-}h}$, and band gap ΔE_{BG} can be related to the chemical disorder in the Si-Ge host matrix. In particular, the disorder generates a distinctive environment around every Be pair, so that each bound exciton has a different exciton binding energy.[27] This variation is given by[8,26]

$$\Delta E_i=2.36\left|\frac{dE_i}{dx}\right|\left[\frac{x(1-x)}{N8\pi R_i^3}\right]^{1/2}, \tag{16}$$

where N is the density of lattice sites, R_i is the Bohr radius of the particle, and $i=e$ and $e\text{-}h$. For the diamond structure, $NR_i^3=8(R_i/a)^3$, where a is the lattice constant of the strained alloy.

Using $dE_{\text{BG}}/dx=412\text{–}440x$ meV (for the unstrained alloy) and $R=5.1$ Å, $\Delta E_{\text{BG}}=18$ meV (for $x=0.08$). (For the undoped alloy, $R=38$ Å, which leads to $\Delta E_{\text{BG}}=\sim1$ meV, which is a small fraction of the 7-meV PL linewidth for the undoped alloy.[9]) For electron trapping, $dE_e/dx=-212$ meV (see Sec. III A 1, with $m_h=0.38m_0$), so with $R_e=5.1$ Å (Ref. 5) and $E_e=31$ meV, $\Delta E_e=10.5$ meV. For hole trapping, $dE_{e\text{-}h}/dx=-50$ meV (see Sec. III A 1), so, with $R_{e\text{-}h}=20$ Å,[5] $\Delta E_{e\text{-}h}=3.0$ meV. Assuming inhomogeneity with a Gaussian distribution, the total linewidth of the zero-phonon peak in the Be-doped alloy is

$$\Delta E^G=(\Delta E_{\text{BG}}^2+\Delta E_e^2+\Delta E_{e-h}^2)^{1/2}. \tag{17}$$

Equation (17) gives $\Delta E^G=20.8$ meV, which is roughly equal to the 22-meV linewidth in the epilayer.

In the SL's there is additional spatial inhomogeneity in $E_{e\text{-}h}(\Delta E_{e,h}^{\text{Be}})$ due to the spatial profile of the Be dopant (Fig. 8), which is the standard variation of $E_{e\text{-}h}$ within the Be profile. For SL-*A*, SL-*B*, and SL-*C*, $\Delta E_{e,h}^{\text{Be}}$ is estimated to be 2, 3, and 5 meV, respectively. This contribution is small, and the widths of the epilayer and SL's are expected to be nearly the same.

Another possible source of broadening is due to strain in the Be pairs. In unstrained Si:Be, the substitutional-interstitial Be pair has a compressive strain of $\sim3.4\times10^{-4}$ along the [111] direction of the pair.[23] This leads to a 4-meV splitting of the A and B' lines in Si:Be (which are not resolved in SiGe:Be), and may lead to up to $\sim$4 meV broadening in the alloy. This is an upper limit because there are B and B'' peaks between A and B', and the peaks often have different heights. For the strained $\text{Si}_{0.92}\text{Ge}_{0.08}$:Be epilayer, $\varepsilon_{xx}=\varepsilon_{yy}=-3.3\times10^{-3}$ and $\varepsilon_{zz}=+2.6\times10^{-3}$, which project to give a compressive strain of -1.3×10^{-3} along [111]. If it is assumed that this causes a total strain of -3.3×10^{-3} on the Be_2 pair (which would be reasonable for equal bulk moduli for the lattice and Be_2), the A/B' splitting would be $\sim$16 meV. This would lead to additional homogeneous broadening with an upper limit of $\sim$16 meV (given equal A and B' peak heights), which could be a significant component of the total linewidth. However, this does not seem to be significant for two reasons. The decrease in linewidth with increasing pressure (Sec. II) is much larger than that predicted using this result, which is only $\sim$1 meV from 1 bar to 50 kbar, with these upper-limit values. Also, given the inhomogeneity of the pore sizes for the interstitial Be atoms available in the alloy, it seems unlikely that very highly strained Be pairs would form during doping, especially with *in situ* doping.

B. PL at elevated pressure

Application of hydrostatic pressure to strained SiGe:Be heterostructures can affect PL in several ways. The decrease in volume changes the SiGe band gap (E_{BG}) and the trapping of the electrons to the Be pair (E_e).[5] Reference 5 suggests that such a volume change will have little effect on electron-hole binding (E_{e-h}); also, the effect of pressure on the dielectric constant and particle mass is small.[10] Pressure may have a small influence on confinement energies. Furthermore, the applied pressure decreases the biaxial strain in the alloy layer, and this will alter the average energies and splittings of the hole and electron bands. The changed biaxial strain may also affect the strain on the Be pairs, which can also affect PL emission. Changes in the hydrostatic and nonhydrostatic components of strain can also modify the conduction- and valence-band offsets at the superlattice interfaces.

The band gap of unstrained $Si_{0.92}Ge_{0.08}$ at pressure P (in kbar) is

$$E_{BG}(P)=E_{BG}(P=1\ \text{bar})+(dE_{BG}/dP)P. \tag{18}$$

Since $dE_{X-\Gamma}/dP$ is -1.50 meV/kbar for both Si and Ge,[28] dE_{BG}/dP is assumed to be -1.50 meV/kbar for the alloy. Therefore, the changes in the band gap are the same in unstrained Si:Be and $Si_{0.92}Ge_{0.08}$:Be as pressure is applied.

For low pressures, the nonhydrostatic strain components are

$$\varepsilon_{xx}^{(b)}(P)=\varepsilon_{yy}^{(b)}(P)=\frac{a_{Si}}{a}\left(\frac{1-\dfrac{P}{3B_{Si}}}{1-\dfrac{P}{3B}}\right)-1=\varepsilon^{(b)}(P), \tag{19}$$

$$\varepsilon_{zz}^{(b)}(P)=-\frac{2C_{12}}{C_{11}}\,\varepsilon_{xx}^{(b)}(P), \tag{20}$$

where B and B_{Si} are the bulk moduli of the epilayer and the substrate Si, respectively, and a and a_{Si} are the lattice constants of the epilayer and the substrate Si, respectively (Table III).[17] The shifts in the hole and conduction bands due to biaxial strain at different pressure are obtained from Eqs. (5)–(7) and (8) and (9), respectively, using Eq. (19); the change due to contracted volume is similarly obtained by using Eq. (4).

The band gap at pressure P is then

$$E_{BG,hh(lh)}(P)=E_{BG}(P)+\Delta E_{BG}^{\varepsilon}(P) -\Delta E_c^{100,010}(P)-\Delta E_{hh(lh)}(P). \tag{21}$$

Figure 3 plots the band gap (E_{BG}) of the unstrained $Si_{0.92}Ge_{0.08}$ alloy, and gaps between the hole bands and the lowest conduction band ($E_{BG,hh}$ and $E_{BG,lh}$) for the strained alloy. $dE_{BG,hh}/dP$ ($=-1.38$ meV/kbar) and $dE_{BG,lh}/dP$ ($=-1.43$ meV/kbar) are smaller in magnitude than that for the unstrained alloy dE_{BG}/dP ($=-1.50$ meV/kbar for unstrained Si and $Si_{0.92}Ge_{0.08}$). These slopes of the two band gaps are in good agreement with that determined from zero-phonon emission in $Si_{0.75}Ge_{0.25}$/Si strained quantum wells ($dE_{PL}/dP=-1.40$ meV/kbar).[29]

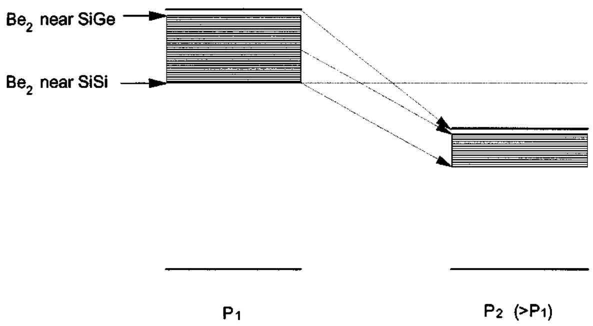

FIG. 9. A schematic energy diagram for the distribution of electron binding energies E_e at two pressures.

1. Zero-phonon emission from the epilayer

The change in the energy of the zero-phonon emission in the strained $Si_{0.92}Ge_{0.08}$:Be alloy is similar to that of the *A* line in bulk Si:Be. Both decrease linearly with pressure with approximately the same slope; the pressure dependence of the *B* line in Si:Be is more quadratic, and has a steeper slope.[5] The magnitude of the pressure coefficient of the PL peak in the strained $Si_{0.92}Ge_{0.08}$:Be epilayer ($dE_{PL}/dP=-0.68$ meV/kbar) is actually slightly smaller than that for the *A* peak in Si:Be ($dE_{PL}/dP=-0.77$ meV/kbar), by 0.09 meV/kbar. Within experimental error this can be attributed to the smaller magnitude of α for the hh band gap in the strained alloy *vis à vis* the band gap in the unstrained alloy (by 0.12 meV/kbar).

Another factor that can contribute to this difference comes from the model presented in Sec. III A 3 (Figs. 9 and 10) describing the inhomogeneous distribution of binding energies for electron trapping. This model predicts significant line-shape broadening at ambient pressure. The decrease in PL linewidth and intensity with increasing pressure, along with the decreasing E_e with increasing Ge content (x) in the alloy, all suggest that the binding energies in SiGe:Be range from that in Si:Be to values near zero. Since added pressure

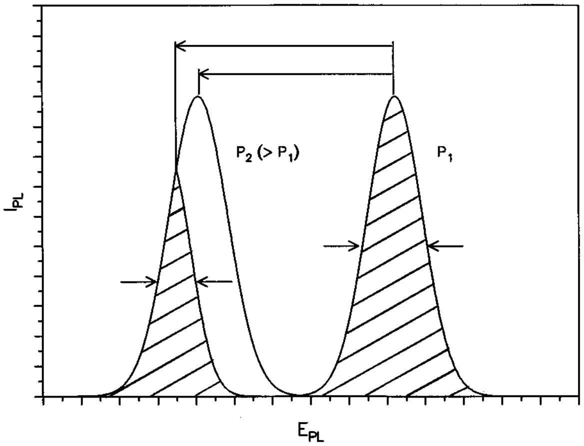

FIG. 10. The simulated photoluminescence spectrum I_{PL} (hatch marked region), using Fig. 9 and the model presented in Sec. III A 3.

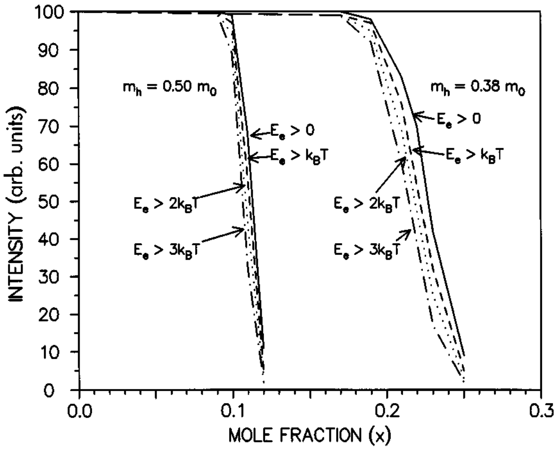

FIG. 11. The simulated integrated PL intensity as a function of the mole fraction.

decreases the binding energy of each site, the less strongly a site binds electrons at ambient pressure, the lower the pressure that needs to be applied to prevent electron trapping at that site. While α determined above, which includes effects due to changing biaxial strain, would characterize any given Be_2 trap, the peak of the measured PL (due to recombination at all traps remaining at pressure P) would apparently decrease even faster (Fig. 10) with a magnitude that is larger by about half the rate the FWHM decrease with P, or about an additional 0.05 meV/kbar. Still, the measured value α for the epilayer is consistent with expectations, within experimental error. Quantitative predictions of this model give $\alpha = -0.86$ meV/kbar for $m_h = 0.38 m_0$ (see Sec. III C).

2. Zero-phonon emission from SL-A

The PL peak decreases in energy with increasing pressure faster in SL-A ($\alpha = -0.97$ meV/kbar) than in the epilayer ($\alpha = -0.68$ meV/kbar). The difference in these values of α is larger than experimental error. One possible reason for this difference is the changing hole confinement in the SL with pressure. The effective mass of the heavy hole is fairly independent of the pressure, while the well width decreases by 0.02 Å/kbar. The change of α due to the change in the confinement energy from the reduced width of the well is -0.01 meV/kbar. Contributions attributable to pressure-induced changes in the valence-band offset will be similarly small. The different distributions of Be in the epilayer and SL-A seem to lead to different values of α. Since the band offset of the conduction band is negligible in the SL, the energy of (free) electrons is the same in both the Be-doped epilayer and SL, and will not cause α to have different values. The model prediction in Sec. III C of $\alpha = -0.86$ meV/kbar ($m_h = 0.38 m_0$) is actually in between the values for the epilayer and SL-A.

3. PL linewidth and intensity

The linewidths of the zero-phonon PL peak in the strained epilayer and SL-A decrease from 22 and 21 meV, respectively, at ambient pressure to 16 meV at 50 kbar (for the epilayer, see Fig. 4). The model presented in Sec. III C suggests that ΔE_e decreases from 10.5 meV to ~0 as pressure increases from 1 bar to 58 kbar, where PL is no longer seen. Using Eq. (17), this would decrease the observed linewidth by ~3 meV, which is about half of the observed decrease. If the broadening profile were not Gaussian, but had more Lorentzian character, the decrease predicted by the model would be even larger.

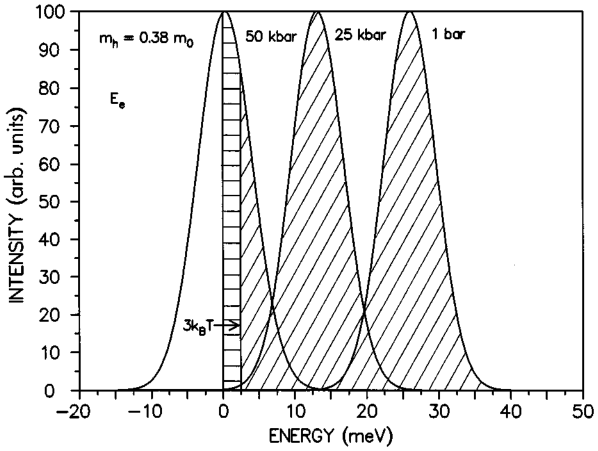

FIG. 12. The simulated distribution of electron binding energies E_e at 1 bar, 25 kbar, and 50 kbar ($m_h = 0.38 m_0$). Note the negative energies denote unbound states, and the hatch marks indicate states with binding energy $> 3k_BT$.

PL from the epilayer and SL-A decreases roughly linearly with increasing pressure, becoming zero near ~58 kbar, while in Si:Be the integrated PL remains roughly constant up to ~50 kbar and decreases abruptly at higher pressure. These differences can be explained by differences in exciton binding. In Si:Be there is a single type of binding site, and in SiGe:Be there is a distribution of binding sites, as is detailed in Sec. III C.

4. TO-phonon replica of free excitons in Si and the "new" peak at high pressure

The PL feature in SL-A attributed to TO-phonon replicas of free excitons in Si shifts toward lower energy with added pressure (up to 54 kbar) at a rate slightly higher than that of the band gap of bulk Si (Fig. 3). Above 54 kbar, the magni-

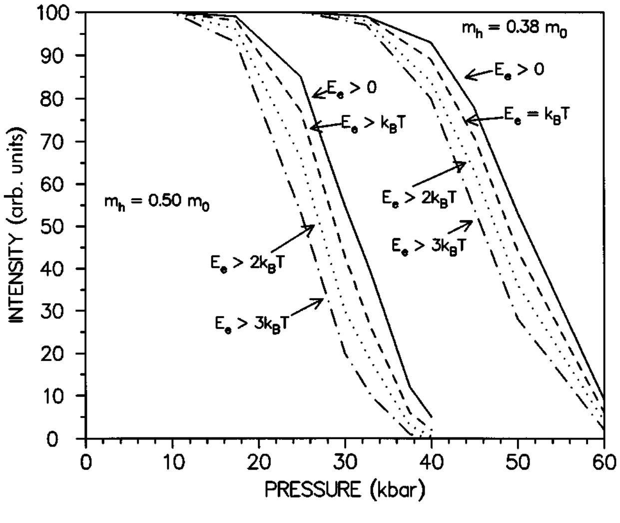

FIG. 13. The simulated integrated PL intensity as a function of pressure.

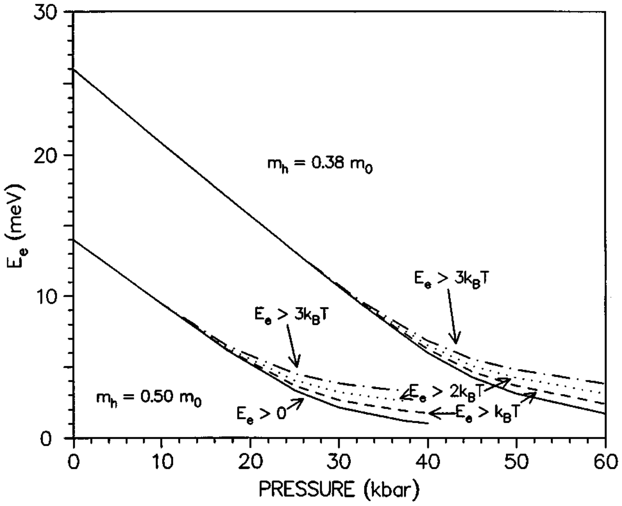

FIG. 14. The simulated average electron binding energy E_e as a function of pressure.

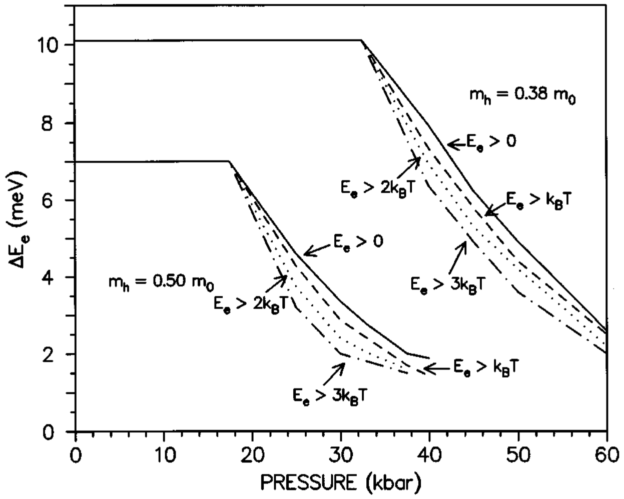

FIG. 15. The simulated linewidth contribution ΔE_e to the PL linewidth as a function of pressure.

tude of α for this peak increases dramatically by an order of magnitude (Fig. 3). These TO-phonon replicas may be too weak to be detected at high pressures in the other Be-doped samples (the SL's, the epilayer, and bulk Si). Since this dramatic change in SL-A occurs at pressures where excitons no longer bind to the Be complex, the origin of the peak may have some relation to the existence of Be impurities.

C. Inhomogeneous distribution of exciton binding energies

Small variations in the potential that binds an electron to a Be pair can lead to significant changes in E_e. For example, in the double-potential-well binding model for Si:Be presented in Ref. 5 (model A), a well binds an electron to each Be atom with well depth V_{Si} of 6.167 eV at ambient pressure. This well depth leads to a binding energy E_e=48 meV; no binding occurs for well depths <5.831 eV. If the well width in the alloy a_0 scales with the average bond distance in the alloy, $a_0(x)=1.18$ Å $(1+0.024\,x)$, and the bond distance of the Be pair d_0 is fixed at 1.9 Å, then $d\langle E_e(x)\rangle/dx=-212$ meV (for $m_h=0.38m_0$) results in an average binding potential in the alloy of $\langle V_{\mathrm{SiGe}}(x)\rangle=6.167\,(1-0.27x)$ eV. [For $m_h=0.50m_0$, $\langle V_{\mathrm{SiGe}}(x)\rangle=6.167(1-0.62x)$ eV.] Since there is a distribution of E_e for a given x, the average value of the electron binding energy is now written explicitly as $\langle E_e(x)\rangle$. Although $\langle E_e(x)\rangle$ reaches zero for $x=0.23$, some binding sites are available for silicon-rich alloys with this, and somewhat larger values of x because of this distribution.

The model in Sec. III A 3 suggests that the contribution to the PL linewidth at ambient pressure from spatial variation is $\Delta E_e(x)=38.7\sqrt{x(1-x)}$ meV for $m_h=0.38m_0$, which is 10.5 meV for $x=0.08$. This is the FWHM of electron binding energies. Assuming that $a_0(x)$ and d do not vary throughout a given alloy, this form for $\Delta E_e(x)$ results in a Gaussian distribution of binding potential depths with FWHM $\Delta V_{\mathrm{SiGe}}(x)=-3.77x^2+1.34$ eV. [For $m_h=0.5m_0$, $\Delta E_e(x)=26.2\sqrt{x(1-x)}$ meV, $\Delta E_e(0.08)=7.1$ meV, and $\Delta V_{\mathrm{SiGe}}(x)=-3.10x^2+1.21$ eV.]

If the photoluminescence intensity (I_{PL}) is proportional to the density of sites with $E_e \geqslant k_BT$ (say with $E_e \geqslant 0-3k_BT$) and the density of Be_2 pairs is independent of x, this model [using $\langle V_{\mathrm{SiGe}}(x)\rangle$ and $\Delta V_{\mathrm{SiGe}}(x)$] predicts that at ambient pressure I_{PL} decreases with x, as shown in Fig. 11, and becomes effectively zero for silicon-rich alloys with $x \geqslant 0.23$ (with $m_h=0.38m_0$), as has been observed experimentally.[1] Because only silicon-rich alloys ($x<0.5$) are being analyzed here, no conclusions can be drawn concerning emission from Be-doped germanium-rich alloys and germanium.

Adopting an approach similar to that in Ref. 5, when pressure is applied $a_0(x)$ and d both decrease by the factor $(1-P/3B_{\mathrm{Si}})$, and the depth of each potential well does not change. Therefore, $\langle\Delta V_{\mathrm{SiGe}}(x)\rangle$ and $\Delta V_{\mathrm{SiGe}}(x)$ do not vary with P. Then the distribution of $E_e(x)$ can be determined at arbitrary P, and the photoluminescence profile can be determined by including only sites with $E_e(x) \geqslant E_{\mathrm{min}}$ (which could be $0-3k_BT$). The value of $I_{\mathrm{PL}}(x)$ can then be tracked with pressure, and the shift of the peak of the PL spectrum due to the changing distribution of binding sites can be calculated (Figs. 9 and 10). This distribution of sites is illustrated in Fig. 12. For strained $\mathrm{Si}_{0.92}\mathrm{Ge}_{0.08}$, the change in the integrated intensity with pressure is shown in Fig. 13; the binding energy E_e and linewidth contribution ΔE_e are plotted in Figs. 14 and 15, respectively. Figures 13–15 are shown for $m_h=0.38m_0$ and $0.50m_0$. The model with the heavy-hole mass $(0.50m_0)$ averaged over angle seems to fit the observed changes of PL with pressure better, although both fits are qualitatively reasonable.

The values of α $(=dE/dP)$ for the epilayer and SL-A can be predicted using this model, with $\alpha=dE_{\mathrm{BG,hh}}/dP-dE_e/dP$. The first contribution is -1.38 meV/kbar, and dE_e/dP is the slope of the curves in Fig. 14, which is (at low pressure) 0.52 meV/kbar for $m_h=0.38m_0$ and 0.45 meV/kbar for $m_h=0.50m_0$. This gives -0.86 and -0.93 meV/kbar, respectively, which fall in between the measured values of α for the epilayer and SL-A.

IV. CONCLUDING REMARKS

Photoluminescence in a strained SiGe alloy isoelectronically doped by Be atom pairs can be understood by separately examining the effects of alloying on the band gap, strain (due to commensurate growth and applied hydrostatic pressure), confinement, and exciton binding. Exciton binding depends on how the structure is doped by Be, how electrons are trapped by Be_2, and how the holes are bound to the trapped electrons. It appears that electron trapping in Be-doped SiGe alloys is similar to that in Si:Be, except that there is an inhomogeneous distribution binding potential (even on a microscopic scale) in the alloy that leads to spread in exciton binding energies. This picture explains many of the observations, including the decrease in the linewidth of zero-phonon PL in $Si_{0.92}Ge_{0.08}$:Be at elevated pressure.

ACKNOWLEDGMENTS

This work was supported at Columbia University (S.K., G.C., and I.P.H.) by the Joint Services Electronics Program Contract No. DAAH04-94-G-0057 and at the University of Rochester (K.L.M. and D.G.H.) by the U.S. Air Force Office of Scientific Research Contract No. F49620-92-J-0336.

---

[1] R. A. Modavis, D. G. Hall, J. Bevk, B. S. Freer, L. C. Feldman, and B. E. Weir, Appl. Phys. Lett. **57**, 954 (1990).

[2] R. A. Modavis, D. G. Hall, J. Bevk, and B. S. Freer, Appl. Phys. Lett. **59**, 1230 (1991).

[3] K. L. Moore, O. King, D. G. Hall, J. Bevk, and M. Furtsch, Appl. Phys. Lett. **65**, 2705 (1994).

[4] S. S. Iyer and Y.-H. Xie, Science **260**, 40 (1993).

[5] S. Kim, I. P. Herman, K. L. Moore, D. G. Hall, and J. Bevk, Phys. Rev. B **53**, 4434 (1996).

[6] J. J. Hopfield, D. G. Thomas, and R. T. Lynch, Phys. Rev. Lett. **17**, 312 (1966).

[7] A. Hartman, L. Vescan, C. Dieker, T. Stoica, and H. Lüth, Phys. Rev. B **48**, 18 276 (1993).

[8] N. L. Rowell, J.-P. Noël, D. C. Houghton, A. Wang, L. C. Lenchyshyn, M. L. W. Thewalt, and D. D. Perovic, J. Appl. Phys. **74**, 2790 (1993); J. Hartung, V. Higgs, G. Davies, E. C. Lightowlers, V. Arbet-Engel, and K. L. Wang, Jpn. J. Appl. Phys. **33**, 2340 (1994).

[9] J. Weber and M. I. Alonso, Phys. Rev. B **40**, 5683 (1989).

[10] Y. Shiraki and S. Fukatsu, Semicond. Sci. Technol. **9**, 2017 (1994).

[11] D. J. Robbins, L. T. Canham, S. J. Barnett, A. D. Pitt, and P. Calcott, J. Appl. Phys. **71**, 1407 (1992).

[12] W. T. Masselink and Y.-C. Chang, Phys. Rev. Lett. **51**, 506 (1983).

[13] H.-J. Müller and H.-J. Wünsche, Phys. Status Solidi B **124**, 747 (1984).

[14] R. People, Phys. Rev. B **42**, 1405 (1985); D. V. Lang, R. People, J. C. Bean, and A. M. Sergent, Appl. Phys. Lett. **47**, 1333 (1985).

[15] C. G. Van de Walle and R. M. Martin, Phys. Rev. B **34**, 5621 (1986); G. C. Van de Walle, Phys. Rev. B **39**, 1871 (1989).

[16] D. Dutartre, G. Brémond, A. Souifi, and T. Benyattau, Phys. Rev. B **44**, 11 525 (1991).

[17] J. A. Tuchman, S. Kim, Z. Sui, and I. P. Herman, Phys. Rev. B **46**, 13 371 (1992); J. A. Tuchman and I. P. Herman, *ibid.* **45**, 11 929 (1992); J. A. Tuchman, Z. Sui, S. Kim, and I. P. Herman, J. Appl. Phys. **73**, 7730 (1993).

[18] J. K. Ord, *Families of Frequency Distributions* (Griffin, London, 1972), p. 101.

[19] R. People, IEEE J. Quantum Electron. **QE-22**, 1696 (1986).

[20] K. Tanaka, M. Nagaoka, and T. Yamabe, Phys. Rev. B **28**, 7068 (1983).

[21] J. M. Shi, F. M. Peeters, and J. T. Devreese, Phys. Rev. B **50**, 15 182 (1994).

[22] G. Bastard, J. A. Brum, and R. Ferreira, in *Solid State Physics*, edited by H. Ehrenreich and D. Turnbull (Academic, Boston, 1991), Vol. 44, p. 229.

[23] G. Bastard, Phys. Rev. B **24**, 4714 (1981).

[24] H. Navarro-Contreras, R. A. Brito-Orta, T. Timusk, W. R. Datars, and D. C. Houghton, Solid State Commun. **90**, 311 (1994).

[25] A. Kahan, M. Chi, and L. Friedman, J. Appl. Phys. **75**, 8012 (1994).

[26] J. M. Langer, R. Buczko, and A. M. Stoneham, Semicond. Sci. Technol. **7**, 547 (1992); R. Benzaquen, S. Chrbonneau, N. Sawadsky, A. P. Roth, R. Leonelli, L. Hobbs, and G. Knight, J. Appl. Phys. **75**, 2633 (1994).

[27] H.-J. Muller, Phys. Status Solidi B **132**, 239 (1985).

[28] R. D. Hong, D. V. Jenkins, S. Y. Ren, and J. D. Dow, Phys. Rev. B **38**, 12 549 (1988).

[29] G. A. Northrop, J. F. Morar, D. J. Wolford, and J. A. Bradley, Appl. Phys. Lett. **61**, 192 (1992).